References

FUJII, S., HAMADA, K., MIURA, R., UESUGI, S., IKEHARA, M. & TOMITA, K. (1982). *Acta Cryst.* B**38**, 564–570.

HAMADA, K., MATSUO, Y., MIYAMAE, A., FUJII, S. & TOMITA, K. (1982). *Acta Cryst.* In the press.

IKEHARA, M., KANEKO, M., MUNEYAMA, K. & TANAKA, H. (1967). *Tetrahedron Lett.* **40**, 3977–3982.

International Tables for X-ray Crystallography (1974). Vol. IV. Birmingham: Kynoch Press.

MAIN, P., HULL, S. E., LESSINGER, L., GERMAIN, G., DECLERCQ, J.-P. & WOOLFSON, M. M. (1978). *MULTAN 78. A System of Computer Programs for the Automatic Solution of Crystal Structures from X-ray Diffraction Data.* Univs. of York, England, and Louvain, Belgium.

PATTABIRAMAN, N., RAO, S. N. & SASISEKHARAN, V. (1980). *Nature (London)*, **284**, 187–188.

TANAKA, K., FUJII, S., FUJIWARA, T. & TOMITA, K. (1979). *Acta Cryst.* B**35**, 929–933.

UNICS (1973). *The Universal Crystallographic Computing System.* Library of Programs, Computation Center, Osaka Univ.

Acta Cryst. (1982). B**38**, 1942–1952

The Charge Density in Polymorph II of 5,5-Diethylbarbituric Acid (Barbital) at 198 K

BY B. M. CRAVEN, R. O. FOX JR AND H.-P. WEBER

Department of Crystallography, University of Pittsburgh, Pittsburgh, PA 15260, *USA*

(*Received* 6 *July* 1981; *accepted* 6 *January* 1982)

Abstract

The charge density in barbital II ($C_8H_{12}N_2O_3$) at 198 K has been determined from 3220 X-ray reflections (Mo $K\alpha$ radiation) having $\sin\theta/\lambda < 1{\cdot}08$ Å^{-1} and $|F_{obs}| > 3\sigma$. Atomic positional parameters and H-atom thermal parameters were given fixed values determined in a previous neutron structure determination. Other parameters, including electron population parameters, and third-order temperature factors, were obtained by least-squares refinement, assuming Stewart's rigid pseudoatom formalism. Results show that in chains of four C atoms there appears to be an alternation of atomic charges which may represent an inductive effect. The H atom which is H-bonded is significantly depleted of electronic charge (~0·2 e) compared with methyl or methylene H atoms. There is a polarization of charge density in C—N and C—O bonds. Carbonyl O atoms have paired lobes of excess electron density (~1·2 e Å^{-3}) above and below the amide plane. It has not been explained why these lobes are found in various orientations in amide crystal structures. The calculated molecular dipole moment is 0·7 (1·2) debye (1 debye = 3·336 × 10^{-30} C m) with negative charge displacement towards atom C(5) and positive towards O(2).

Introduction

The barbiturate drugs act primarily on the central nervous system, producing sleep, hypnosis, anesthesia or death. They have both pre- and postsynaptic effects (Nicoll, 1978). The principal postsynaptic effect of barbiturates is to antagonize the excitatory action of neurotransmitters such as acetylcholine and amino acids. Presynaptic effects are poorly understood, but these may include modification of the rate of transmitter release. Barbiturate receptor sites have not yet been identified at the molecular level. Postsynaptic activity seems to be insensitive to the molecular structure of the barbiturate and may occur through nonspecific membrane interactions. Other interactions must involve considerable stereoselectivity, since there are significant differences in the duration of sleep induced by *R*(+)- and *S*(−)-pentobarbital, or secobarbital (Freudenthal & Martin, 1975).

In order for barbiturates to have potent hypnotic activity, they must have amphiphilic properties which are derived from a polar ring system (typically a trioxopyrimidine moiety) and two non-polar C(5) substituents (typically containing a total of from four to eight C atoms). They are weak acids ($pK_a \sim 7{\cdot}5$) which are partially dissociated at pH values corresponding to those of most body fluids.

There have been extensive crystal structure determinations of the barbiturate drugs, which have given a better understanding of their tautomeric form and conformation (Craven, Vizzini & Rodrigues, 1969; Bideau, Leroy & Housty, 1969; Williams, 1974; Voet, 1972), their metal binding (Wang & Craven, 1971) and their characteristic crystal polymorphism (Craven & Vizzini, 1971). The barbiturate drugs are remarkable in

0567-7408/82/071942-11$01.00

forming crystal complexes with a variety of other small molecules. Many of these structures have been determined because they may be relevant to the interactions at barbiturate receptor sites. Notable are the complexes with adenine derivatives in which barbiturates mimic the base-pairing interaction of uracil or thymine (Kim & Rich, 1968). However, H-bonded crystal complexes also form with imidazole (Hsu & Craven, 1974*a*), amides (Gartland & Craven, 1974) and hexamethylphosphoramide (Hsu & Craven, 1974*b*). In all these complexes, barbiturates form short H bonds which involve their NH groups and acceptor N or O atoms from the partner in the complex (Gartland & Craven, 1974; Hsu & Craven, 1974*a*). Conversely, the H bonds between partners involving the barbiturate carbonyl O acceptor atoms tend to be long, if they exist at all. These comparisons are made with respect to the H-bond distances in which barbiturate molecules H bond with each other (Craven, Cusatis, Gartland & Vizzini, 1973). Thus it is concluded that the mechanism of drug action is likely to involve strong H bonding with an acceptor atom of the receptor site.

The determination of the electronic charge-density distribution in barbital (5,5-diethylbarbituric acid, Fig. 1)* may lead to a better understanding of barbiturate molecular interactions. The X-ray diffraction data for four H-bonded crystal complexes of barbital have already been reanalyzed in terms of Stewart's (1970) *L*-shell projection method, so as to obtain estimates of the net atomic charges (Ruble, Wang & Craven, 1979). The results showed an interesting alternation of charges on the barbital C atoms. The H-bonded H atoms were found to be depleted of charge when compared with H atoms bonded to C.

We now report a more detailed study of the charge density in the crystal structure of barbital itself in which we consider the asphericity in the electronic charge distribution about each atom center. Because of the complexity involved, such an analysis should be carried out with a crystal structure which is as simple as possible. We chose barbital because it is the simplest barbiturate having drug action. We chose the crystal polymorph II because in this structure the molecule lies on a twofold crystallographic axis (Craven, Vizzini & Rodrigues, 1969) thus giving a substantial reduction in the number of structure parameters to be determined. It is desirable to collect the diffraction data at low temperature so as to minimize problems in deconvoluting the static charge density from the atomic thermal motion. We have already reported a neutron diffraction study of barbital II at 198 K which was carried out in order to obtain accurate values for nuclear positional and thermal parameters, particularly those for the H atoms (McMullan, Fox & Craven, 1978; hereafter MFC). Efforts to reach temperatures lower than about 175 K were frustrated by the fracture of the large crystals (~4 mm^3) used for neutron work, although smaller crystals of barbital II suitable for X-ray data collection could be cooled to about 110 K without fracture. It was shown by X-ray diffraction that there was no phase change or discontinuity in lattice parameters near 175 K. The X-ray intensity data for the charge-density study were collected at 198 K, in order to match the crystal temperature for the neutron study.

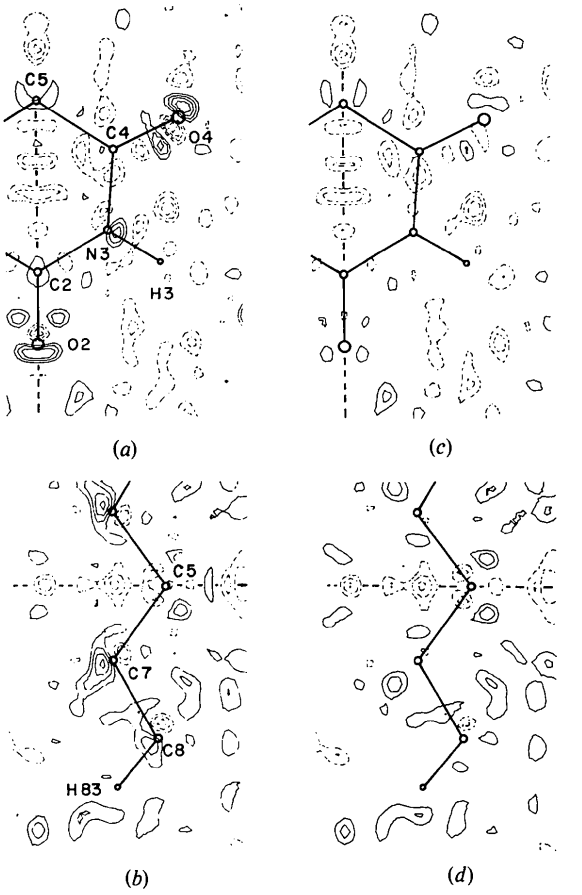

Fig. 1. Atom nomenclature for barbital and difference Fourier syntheses showing the residual charge density. The crystallographic twofold axis is shown as a heavy dashed line. The electron density is shown with contours at intervals of 0·05 e Å^{-3}. Positive regions have solid lines, negative regions have broken lines and the zero contour is omitted. The average e.s.d. in the charge density is 0·05 e Å^{-3}. (*a*) Section in the plane through the ring atoms. (*b*) Section in the best least-squares plane of the ethyl-group C atoms. This plane makes a dihedral angle of 91·0° with the plane in (*a*). (*c*) Section as in (*a*), after the final refinement. (*d*) Section as in (*b*), after the final refinement. The sections (*a*) and (*b*) show significant residual density (~4σ) near several atom centers, which is absent in sections (*c*) and (*d*). This results from including third-order temperature factors in the refinement.

* For further details of barbital atomic nomenclature, molecular conformation and H bonding, see McMullan, Fox & Craven (1978) and Craven, Vizzini & Rodrigues (1969).

Experimental

Prismatic monoclinic crystals of barbital II were grown by slow cooling (~4 h) of a hot saturated ethanolic solution. The two crystals which were used for the X-ray data collection were examined by optical goniometry and shown to have all 14 faces of the forms $\{11\bar{1}\}$, $\{021\}$, $\{110\}$ and $\{010\}$. The X-ray data were measured using an Enraf–Nonius CAD-4 diffractometer with graphite-monochromated Mo $K\alpha$ radiation. The crystal was cooled to 198 ± 2 K by a stream of dry nitrogen gas from an Enraf–Nonius low-temperature device. The temperature was measured using a thermocouple at a distance 8 mm upstream from the crystal.

The crystal lattice parameters were obtained by a least-squares fit to $\sin^2\theta$ values measured at $\pm\theta$ for 15 reflections in the range $18° < \theta < 25°$. The results, which have already been reported by MFC, assumed the Mo $K\alpha$ average wavelength (0·7107 Å). However, Epstein, Ruble & Craven (1982) have since shown that for reflections in this θ range, the appropriate wavelength is that of the α_1 component (0·7093 Å). The revised cell dimensions* for 198 K are thus a = 7·098 (2), b = 14·077 (3), c = 9·726 (1) Å and β = 88·86 (3)°. The crystals have the space group $C2/c$ with four molecules in the unit cell.

X-ray intensity data were collected using $\theta/2\theta$ scans with variable width given by $\Delta 2\theta(°) = 2·0 + 0·9 \tan\theta$ and at a speed so that no more than 2 min were spent on each reflection. The background intensity was estimated from the first and last sixth of each scan. Three standard reflections were remeasured after every fifty reflections. Their intensities varied within 5% of the mean values throughout the two-month period of data collection. Scale factors for individual reflections were estimated by interpolation from the variation in the monitor intensities as a function of time. The variance in an integrated intensity was assumed to be $\sigma^2(I) = \sigma^2 + (0·02I)^2$ where σ^2 is the variance based on counting statistics.

Data collection began with a smaller crystal (0·18 × 0·24 × 0·52 mm) which was mounted with [021] close to the diffractometer φ axis. Before this crystal was lost, 499 reflections were measured, including all those with $\sin\theta/\lambda < 0·35$ Å^{-1}. A larger crystal (0·36 × 0·72 × 0·84 mm) which was mounted with [001] close to the diffractometer φ axis was used to complete the data collection. Because of the large size of this crystal, some photographs were taken at the outset, with X-ray film at the counter window. These were to ensure that no part of the virtual X-ray source or counter window was obscured by the beam pipe system* during an intensity scan. This crystal was used to measure 5579 reflections in the range $0·25$ Å$^{-1} < \sin\theta/\lambda < 1·08$ Å^{-1}. The data from each crystal were reduced to structure amplitudes with inclusion of an absorption correction according to the procedure of Busing & Levy (1957). The absorption coefficient was μ = 0·103 mm^{-1}. For the large crystal the absorption factors for the intensities ranged between 0·942 and 0·969.

The data from the two crystals were combined with a scale factor determined by a least-squares fit (Hamilton, Rollett & Sparks, 1965) using the 286 reflections measured with both crystals. There was a total of 5118 non-symmetry-related reflections, among which 3220 gave $F_{obs} > 3\sigma$. Only the latter were used in the structure refinements.

For the large crystal, the intensity of the 002 reflection, when measured as a function of rotation about the scattering vector, gave systematic variations of 8% from the mean value. This was attributed to extinction, since the variations were considerably larger than a true X-ray absorption effect (1%). Unfortunately, no similar measurements were made with the small crystal before it was lost. However, in the subsequent structure refinements there was no indication that an extinction correction was needed. It appears that by using the intensity data from the smaller crystal for the strong low-angle reflections, the extinction effects have been reduced.

The charge-density refinements

The electronic charge density in the crystal structure was analyzed in terms of the rigid pseudoatom model proposed by Stewart (1976). Pseudoatoms for C, N and O were assumed to have spherical K-shell X-ray scattering factors determined from self-consistent-field wavefunctions (Clementi, 1965). Pseudoatom valence-shell scattering factors were assumed to have radial components derived from Slater-type charge-density functions $[4\pi(n+2)!]^{-1}\alpha^{n+3}r^n \exp(-\alpha r)$ where n = 0, 1, 2 or 3 and α is a radial parameter which is a least-squares variable having different values for C, N, O or H. Explicit functions were the same as those given by Epstein, Ruble & Craven (1982). The angular components describing the pseudoatom asphericity are the terms of a multipole expansion as far as octapoles (or quadrupoles for H) with each term weighted by a population parameter which is a least-squares variable. This introduced sixteen parameters per pseudoatom (nine for H atoms). The structure model also included

* The neutron bond lengths given by MFC should all be reduced by 0·998, since these were calculated assuming the original X-ray cell dimensions. The bond angles are unchanged. The revision of the cell dimensions changes none of the conclusions drawn by MFC, except that there is now less reason to believe that there is a slight difference in crystal temperature between the X-ray and neutron measurements.

* The pipes for the incident beam which were supplied with the instrument did not meet this requirement. Another pipe was specially made.

the usual overall scale factor, atomic positional parameters and anisotropic thermal parameters. Positional parameters for all atoms and anisotropic thermal parameters for the H atoms were assumed to have fixed values determined from the neutron structure determination (MFC). Taking into account the three atoms C(5), C(2) and O(2) which are in special positions on the crystallographic twofold axis, this gave a total of 203 variables to be determined from 3220 observations.

The least-squares refinement was carried out by the computer program of Craven & Weber (1977). The expression to be minimized was $\sum w\Delta^2$, where $\Delta = |F_o| - |F_c|$ and $w = \sigma^{-2}(F_o)$. Convergence was obtained with $R = 0{\cdot}039$, $R_w = 0{\cdot}030$ and QME = 1·37.* The observed value for the total valence charge on the molecule was $\sum p_v = 71{\cdot}1\ (3)$ e. This is in good agreement with the value (72) required for a neutral molecule. In subsequent cycles of refinement the value of $\sum p_v$ was constrained to be 72, thus eliminating the scale factor as an independent variable. There were no resulting significant changes in the parameter values or in the refinement criteria. The final difference Fourier synthesis from this refinement is shown in Fig. 1(*a*) and (*b*). Maps of the static valence-charge distributions and the corresponding deformation charge density are shown in Figs. 2 and 3. In Fig. 1(*a*) and (*b*), the most significant residual charge density (4σ) is found at the peak and trough which are in the ring plane and close to atom O(4). Similar but less pronounced features occur at atoms N(3) and O(2) and the ethyl-group C atoms. These features all recurred with little change when difference Fourier maps were calculated including only reflections with $\sin\theta/\lambda > 0{\cdot}7$ Å^{-1}. Since the contribution of valence-shell scattering is negligible for such reflections, the significant residual charge density was attributed to a deficiency in modelling the observed charge density in regions close to the atom centers.

* $R = \sum|\Delta|/\sum F_o$; $R_w = (\sum w\Delta^2/\sum wF_o^2)^{1/2}$; QME = $[\sum w\Delta^2/(n_o - n_p)]^{1/2}$.

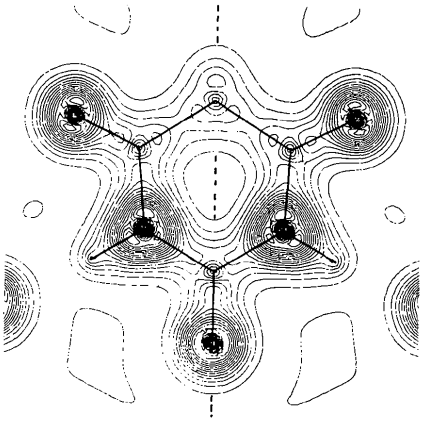

Fig. 2. Total valence-shell charge density for the molecule at rest. The section is the same as in Fig. 1(*a*). Contours are at intervals of 0·5 e Å^{-3}. The maximum value of 8·8 (1) e Å^{-3} is near atom N(3). Note that except at the H atoms where the density is 0·31 (7) e Å^{-3} the atom centers are at local minima in the charge density.

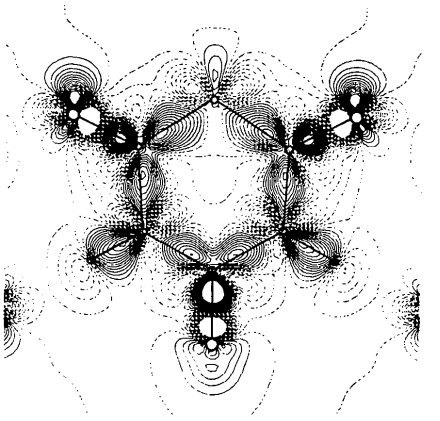

Fig. 3. Map of deformations in the valence charge density. This corresponds to the map in Fig. 2, except that monopole terms are omitted. The charge density in Figs. 2 and 3 comes from the refinement without third-order temperature factors. Contours are at intervals of 0·05 e Å^{-3} with regions of electronic charge deficiency shown as dashed lines. The maximum and minimum values are +1·31 (8) and −1·7 (12) e Å^{-3}, which occur along the C(2)–O(2) bond. Other peaks in the density distribution have e.s.d.'s of 0·04 e Å^{-3}.

The residual features might be due either to a polarization of the static charge density of the core region of the pseudoatoms (Bentley & Stewart, 1974) or to the neglect of curvilinear or anharmonic thermal vibrations in the determination of the nuclear positions from the neutron data (Willis & Pryor, 1975). There may also be some combination of these effects. Further refinements were carried out in an effort to test these notions. They conformed to the procedure adopted in the case of parabanic acid where similar residual-density features were observed close to the center of each O atom (Craven & McMullan, 1979).

The results were difficult to interpret when deformations of the barbital O atom core density were included in the model. Core deformations were introduced as an additional set of three dipole population parameters for each O atom. These parameters were associated with an additional radial function having a large initial exponent ($\alpha = 10$ bohr^{-1}) (the Bohr radius is 52·92 pm) so as to affect the density in the core region of the O pseudoatoms. The refinement converged with an improvement in agreement, giving $R = 0{\cdot}037$, $R_w = 0{\cdot}028$ and QME = 1·31. The final value for the added O radial exponent was $\alpha = 12\ (2)$ bohr^{-1} while the value for the original valence-shell exponent was essentially unchanged, 4·51 (1) bohr^{-1}. The only significant changes in population parameters involved the O dipole deformations. For atom O(2), values of d_1,

d_2, d_3 were 0·04 (2), 0, 0 for the valence-shell dipole and 0·08 (1), 0, 0 for the core. For O(4) these values were 0·02 (1), 0·01 (1), −0·05 (1) and −0·05 (1), 0·05 (1) and 0·05 (1). In contrast to the case of parabanic acid where the sharp and diffuse dipole deformations at each O were oppositely directed, in barbital they do not appear to be correlated in a physically meaningful way. Refinements of this kind were discontinued.

The possibility of improving the description of atomic thermal motion was then tested by first carrying out a new refinement using the neutron data of MFC in order to determine the third-order thermal-vibration parameters, c_{jkl} (Johnson & Levy, 1974) for each atom nucleus. Significantly non-zero values of c_{jkl} were obtained for ring atoms N(3), O(4) and for methyl-group atoms C(8), H(82) and H(83). However, for a given nucleus, the positional parameters (x,y,z) were found to be very strongly correlated with the thermal parameters (c_{111}, c_{222}, c_{333} respectively). Correlation factors ranged from 0·80 to 0·86. Thus it appeared that the nuclear positional parameters could be assigned suitable fixed values with little effect on the refinement criteria. The positional parameters were returned to the fixed values determined by MFC in refinements using only U_{ij} temperature factors. When c_{jkl} parameters were introduced, the R-factor ratio test (Hamilton, 1974) indicated that there was an improvement in the model which could be accepted at the 99·5% level of confidence. In this refinement, the value of R_w was reduced from 0·036 to 0·033, with R = 0·052 and QME = 1·13. The resulting c_{jkl} values are given in Table 2. As expected, when the nuclear positional parameters were included as variables once again, the effect on the refinement criteria was smaller (R_w = 0·032) giving an improvement in the model which was acceptable at a lower confidence level (90%).

If the residual-density features (Fig. 1*a* and *b*) are due to thermal-vibration effects, and if the core electronic charge density follows the nucleus in its thermal motion, then values of c_{jkl} obtained from the neutron data should be very similar to those obtained from the X-ray data with $\sin\theta/\lambda > 0{\cdot}7$ Å^{-1}. Further X-ray refinement was carried out using only the 2068 X-ray reflections with $\sin\theta/\lambda > 0{\cdot}7$ Å^{-1}, and neglecting any contribution to the calculated structure

Table 1. *Anisotropic thermal parameters, U_{ij}*

The temperature-factor expression is $T = \exp(-2\pi^2 \sum_i \sum_j h_i \times h_j a_i^* a_j^* U_{ij})$. Values of U_{ij} ($\times 10^4$ Å^2) are given for all atoms as obtained in the new refinements using the neutron data of MFC, which also included c_{jkl} parameters (Table 2). The second U_{ij} value for each non-H atom is from the refinement using X-ray data.

	U_{11}	U_{22}	U_{33}	U_{12}	U_{13}	U_{23}
C(2)	223 (5)	180 (5)	193 (5)	0	−71 (3)	0
	196 (2)	128 (2)	159 (2)		−75 (2)	
O(2)	382 (7)	170 (6)	357 (7)	0	−156 (5)	0
	319 (4)	133 (2)	290 (3)		−131 (3)	
N(3)	269 (3)	183 (3)	216 (3)	14 (2)	−118 (2)	2 (2)
	239 (2)	144 (1)	171 (2)	11 (1)	−116 (1)	5 (1)
H(3)	458 (9)	301 (8)	350 (8)	47 (6)	−183 (7)	18 (6)
C(4)	234 (4)	185 (3)	180 (3)	11 (2)	−93 (3)	−9 (2)
	205 (2)	144 (1)	141 (1)	10 (1)	−96 (1)	−12 (1)
O(4)	438 (6)	227 (4)	299 (5)	23 (4)	−238 (4)	−27 (3)
	383 (3)	179 (2)	245 (2)	16 (2)	−219 (2)	−29 (2)
C(5)	208 (4)	184 (5)	166 (4)	0	−68 (3)	0
	185 (2)	133 (2)	125 (2)		−62 (2)	
C(7)	338 (4)	272 (4)	276 (4)	105 (3)	−51 (3)	−42 (3)
	302 (2)	236 (2)	220 (2)	106 (2)	−50 (2)	−45 (2)
H(71)	589 (12)	490 (11)	516 (11)	248 (9)	−135 (9)	37 (9)
H(72)	691 (13)	442 (10)	499 (11)	62 (10)	−113 (9)	−188 (9)
C(8)	407 (6)	617 (8)	499 (7)	130 (6)	171 (5)	6 (6)
	371 (4)	571 (6)	429 (5)	126 (4)	159 (4)	0 (5)
H(81)	621 (17)	1207 (30)	1056 (27)	−356 (19)	235 (17)	−126 (22)
H(82)	842 (20)	1058 (24)	717 (19)	194 (17)	269 (16)	385 (17)
H(83)	817 (19)	1104 (27)	1038 (24)	380 (19)	481 (18)	−42 (20)

Table 2. *Third-order atomic thermal parameters, c_{jkl}*

The temperature-factor expression is $T = 1 - \frac{4}{3}\pi^3 i \sum_j \sum_k \sum_i h_j h_k h_i c_{jkl}$. For each parameter, the first value is from the neutron data ($\sin\theta/\lambda \leqslant 0{\cdot}7$ Å^{-1}) and the second (for non-H atoms) is from the X-ray data ($\sin\theta/\lambda > 0{\cdot}7$ Å^{-1}). E.s.d.'s are in parentheses. All values are $c_{jkl} \times 10^8$, except $\times 10^7$ for H atoms and C(8).

	c_{111}	c_{222}	c_{333}	c_{112}	c_{122}	c_{113}	c_{133}	c_{223}	c_{233}	c_{123}
C(2)	0	2 (9)	0	−33 (24)	0	0	0	0	19 (13)	−22 (13)
		0 (2)		−9 (8)					−8 (4)	−1 (4)
O(2)	0	35 (11)	0	−114 (36)	0	0	0	0	−3 (19)	34 (19)
		−3 (2)		−85 (10)					−13 (5)	32 (6)
N(3)	95 (40)	−11 (5)	19 (14)	11 (16)	−8 (7)	−14 (19)	−34 (14)	−7 (5)	20 (8)	11 (9)
	36 (22)	−1 (1)	0 (6)	−11 (7)	−4 (3)	−2 (11)	−5 (7)	0 (2)	−3 (3)	8 (4)
H(3)	−15 (16)	4 (2)	−6 (5)	−3 (5)	3 (2)	9 (8)	−8 (5)	1 (2)	−3 (2)	4 (3)
C(4)	6 (48)	−28 (7)	−4 (17)	42 (17)	−1 (8)	22 (24)	−9 (18)	−4 (6)	13 (9)	−21 (9)
	18 (19)	0 (2)	3 (6)	7 (6)	−3 (2)	−19 (9)	−5 (6)	−1 (2)	−2 (3)	−15 (3)
O(4)	111 (86)	−17 (9)	19 (28)	75 (28)	22 (13)	−51 (43)	−24 (30)	4 (8)	22 (13)	−59 (15)
	269 (40)	−6 (2)	23 (9)	115 (9)	8 (3)	−75 (21)	14 (13)	−1 (2)	34 (3)	−70 (5)
C(5)	0	3 (9)	0	−1 (24)	0	0	0	0	15 (12)	8 (13)
		−6 (2)		9 (8)					5 (3)	−1 (4)
C(7)	119 (67)	−3 (8)	−16 (26)	31 (23)	−15 (12)	−56 (36)	−2 (24)	12 (9)	11 (12)	−9 (13)
	−24 (31)	12 (2)	7 (9)	30 (10)	10 (4)	25 (16)	15 (10)	−3 (3)	19 (4)	−10 (5)
H(71)	−19 (20)	2 (2)	−2 (8)	7 (8)	9 (4)	3 (10)	−8 (7)	0 (2)	3 (3)	−2 (4)
H(72)	10 (25)	2 (2)	5 (7)	1 (8)	4 (3)	14 (11)	−8 (7)	−2 (2)	−3 (4)	1 (4)
C(8)	14 (10)	2 (2)	5 (5)	2 (4)	−1 (2)	−2 (6)	0 (4)	0 (2)	0 (2)	4 (2)
	−11 (5)	5 (1)	12 (3)	1 (3)	0 (1)	−2 (4)	2 (3)	1 (1)	1 (2)	7 (2)
H(81)	−68 (31)	−19 (8)	6 (22)	12 (15)	29 (10)	−53 (21)	−28 (18)	6 (8)	13 (11)	22 (9)
H(82)	−46 (39)	−7 (6)	30 (13)	−2 (16)	14 (8)	19 (19)	43 (13)	14 (6)	39 (8)	29 (9)
H(83)	−14 (39)	7 (7)	30 (20)	19 (16)	4 (10)	−35 (24)	−6 (19)	5 (7)	3 (10)	25 (10)

Table 3. *Charge-density parameters*

The two values given are for the refinements in which c_{jkl} temperature factors (Table 2) were either neglected (top) or included (below). These parameters occur in expressions for the radial and angular charge-density functions which are given by Epstein, Ruble & Craven (1982).

(*a*) Radial parameters

These are values of α (a.u., bohr^{-1}) for radial functions of the Slater type.

C	N	O	H
3·44 (1)	4·04 (2)	4·54 (1)	2·45 (3)
3·48 (1)	4·05 (1)	4·51 (1)	2·37 (3)

(*b*) Electron population parameters ($\times 10^2$)

Values are referred to a right-handed Cartesian set of molecular axes with x along the C(2) → O(2) direction, and z along the normal to the ring plane. Normalization factors as proposed by Hansen & Coppens (1978) have been applied, so that a value of unity corresponds to the transfer of one electron from the negative to the positive regions of the corresponding charge deformation term.

	p_v	d_1	d_2	d_3	q_1	q_2	q_3	q_4	q_5
C(2)	388 (4)	15 (1)	0	0	25 (2)	0	0	6 (2)	-28 (2)
	371 (4)	9 (1)			14 (2)			6 (2)	−20 (2)
O(2)	608 (3)	17 (1)	0	0	−10 (2)	0	0	13 (2)	15 (2)
	621 (3)	8 (1)			−4 (2)			10 (2)	11 (2)
N(3)	506 (5)	2 (1)	6 (1)	−1 (1)	4 (1)	4 (1)	−3 (1)	6 (1)	9 (1)
	500 (4)	0 (1)	−1 (1)	2 (1)	4 (1)	3 (1)	−2 (1)	6 (1)	9 (1)
H(3)	80 (3)	−8 (1)	−13 (1)	2 (1)	−5 (1)	3 (2)	1 (2)	−3 (2)	3 (1)
	88 (2)	−10 (1)	−17 (1)	2 (1)	−7 (6)	6 (2)	2 (2)	−2 (2)	0 (1)
C(4)	402 (3)	−4 (1)	3 (1)	−2 (1)	−6 (1)	−7 (1)	2 (1)	6 (1)	-22 (1)
	388 (3)	−3 (1)	0 (1)	−1 (1)	−1 (1)	−5 (1)	2 (1)	7 (1)	−18 (1)
O(4)	620 (3)	−6 (1)	9 (1)	0 (1)	14 (1)	9 (2)	−2 (2)	12 (2)	14 (1)
	621 (3)	1 (1)	4 (1)	−2 (1)	12 (1)	5 (2)	−2 (2)	13 (2)	11 (1)
C(5)	400 (2)	−6 (1)	0	0	8 (2)	0	0	6 (1)	14 (2)
	396 (3)	−2 (1)			7 (2)			5 (1)	11 (2)
C(7)	394 (4)	−2 (1)	1 (1)	1 (1)	1 (1)	−2 (2)	−1 (2)	4 (2)	9 (2)
	376 (4)	3 (1)	1 (1)	1 (1)	1 (1)	−2 (2)	0 (2)	5 (2)	11 (2)
H(71)	103 (3)	11 (1)	15 (2)	−1 (2)	0 (2)	9 (2)	0 (2)	5 (2)	−7 (2)
	112 (3)	14 (1)	21 (2)	−2 (2)	−2 (2)	13 (2)	0 (2)	4 (2)	−10 (2)
H(72)	101 (3)	9 (1)	−11 (2)	0 (2)	3 (2)	−8 (2)	−2 (2)	4 (2)	4 (2)
	111 (3)	11 (1)	−15 (2)	−1 (2)	2 (2)	−10 (2)	−2 (2)	5 (2)	1 (2)
C(8)	402 (6)	0 (2)	7 (2)	−4 (2)	2 (2)	3 (3)	7 (3)	7 (3)	11 (3)
	387 (5)	8 (2)	1 (2)	2 (2)	1 (2)	−1 (3)	2 (3)	8 (3)	8 (3)
H(81)	111 (4)	−8 (2)	8 (2)	9 (3)	5 (3)	−8 (3)	−8 (3)	7 (3)	3 (3)
	105 (3)	−4 (2)	5 (2)	8 (2)	6 (3)	−5 (3)	−8 (3)	5 (3)	1 (3)
H(82)	107 (4)	−8 (2)	−11 (2)	1 (2)	−5 (2)	7 (3)	0 (3)	2 (3)	3 (3)
	112 (3)	−9 (2)	−12 (2)	3 (2)	−4 (2)	9 (3)	0 (3)	1 (3)	1 (3)
H(83)	86 (4)	10 (2)	−5 (2)	9 (2)	0 (2)	−6 (3)	−3 (3)	0 (3)	−8 (3)
	104 (3)	17 (2)	−6 (2)	15 (2)	3 (2)	−4 (3)	2 (3)	1 (3)	−3 (3)

	o_1	o_2	o_3	o_4	o_5	o_6	o_7
C(2)	33 (1)	0	0	−2 (2)	−2 (1)	0	0
	25 (1)			−1 (2)	1 (1)		
O(2)	4 (1)	0	0	−2 (1)	−10 (1)	0	0
	2 (1)			1 (1)	−0 (1)		
N(3)	−14 (1)	3 (1)	2 (1)	0 (1)	−4 (1)	−3 (1)	3 (1)
	−14 (1)	2 (1)	1 (1)	0 (1)	−3 (1)	−3 (1)	3 (1)
C(4)	29 (1)	−8 (1)	0 (1)	0 (1)	2 (1)	1 (1)	0 (1)
	25 (1)	−5 (1)	0 (1)	0 (1)	0 (1)	4 (1)	0 (1)
O(4)	−1 (1)	1 (1)	−2 (1)	0 (1)	11 (1)	−4 (1)	−2 (1)
	−3 (1)	1 (1)	−1 (1)	1 (1)	−2 (1)	0 (1)	1 (1)
C(5)	−15 (1)	0	0	0 (2)	−16 (1)	0	0
	−15 (1)			0 (2)	−15 (1)		
C(7)	10 (1)	3 (1)	0 (1)	−1 (1)	19 (1)	1 (1)	−3 (1)
	10 (1)	2 (1)	1 (1)	2 (1)	17 (1)	−2 (1)	−4 (1)
C(8)	−13 (2)	−2 (2)	−6 (2)	5 (2)	−18 (2)	0 (2)	6 (2)
	−14 (2)	−1 (2)	−3 (2)	1 (2)	−11 (2)	2 (2)	8 (2)

factors due to the H atoms and the valence-shell density. It was found that if the positional parameters were variables, the correlation factors between (x,y,z) and (c_{111}, c_{222}, c_{333}) were even larger than in the corresponding neutron refinement, ranging from 0·90 to 0·98. The largest correlations involved atom C(8). Consequently, the atomic positional parameters were returned to the original fixed neutron values of MFC. The X-ray refinement then gave convergence with an appreciable reduction in the refinement criteria, with R_w changing from 0·092 to 0·038 for those reflections with $\sin\theta/\lambda > 0{\cdot}7$ Å^{-1}. Other final values were $R = 0{\cdot}056$ and QME = 1·06.

In comparing the c_{jkl} values in Table 2, it should be noted that the e.s.d.'s for the X-ray values are smaller. This is because the neutron values were determined from 1361 reflections with $\sin\theta/\lambda < 0{\cdot}70$ Å^{-1} while the more precise X-ray values were determined from 2068

reflections with $0{\cdot}70\ \text{Å}^{-1} < \sin\theta/\lambda < 1{\cdot}08\ \text{Å}^{-1}$. The X-ray and neutron values are in satisfactory agreement in the sense that there are few differences which are significant because of the large e.s.d.'s in the neutron values. However, there are some highly significant differences in terms of the smaller e.s.d.'s in the X-ray values. When the fixed neutron c_{jkl} values were included in a charge-density refinement, using all the X-ray data, there was a severe deterioration, with R_w increasing from 0·030 to 0·053. In contrast, when fixed X-ray* values of c_{jkl} were substituted for the corresponding neutron values for all except H atoms, there was an improvement in the agreement which was significant at a confidence level higher than 99·5%. Convergence was obtained with $R = 0{\cdot}035$, $R_w = 0{\cdot}026$ and QME = 1·21. Final parameters from this refinement are in Tables 1, 2 and 3.† A difference Fourier synthesis after this refinement (Fig. 1*c* and *d*) showed no significant residual density. In particular, those features which occur close to the atom centers in Fig. 1(*a*) and (*b*) are absent in Fig. 1(*c*) and (*d*).

Although the model which includes third-order temperature factors gives good agreement with the observed total charge-density distribution for barbital, the physical significance of these parameters remains uncertain. It is believed that their major function is to take into account curvilinear atomic vibrations, such as those involved in rigid-body motion. Vibrations of this kind are significant at 198 K. According to MFC, the neutron U_{ij} values are consistent with the barbital ring system having a maximum r.m.s. rigid-body librational amplitude of 4·8°. The agreement between X-ray and neutron values also supports the notion that the c_{jkl} parameters describe thermal-motion effects, but this is not entirely convincing because of the relatively large e.s.d.'s in the neutron values. It must be recognized that the c_{jkl} values also incorporate the effect of any deformation of the static charge density which may be present in the atomic-core region. In our future studies of this kind, efforts will be made to collect neutron intensity data for reflections extending to larger values of $\sin\theta/\lambda$. This will give rise to more precise c_{jkl} values which are unbiased by any core deformations of the electronic charge density.

The procedure whereby fixed neutron values are used in refinements with X-ray data is susceptible to the effects of systematic errors in both X-ray and neutron data. Thus there are systematic differences in the X-ray and neutron U_{ij} values for barbital (Table 1) which are highly significant in terms of their e.s.d.'s. The differences were so large that no effort was made to maintain fixed neutron U_{ij} values in X-ray refinements, except for those of the H atoms. The smaller X-ray values for U_{ij} may be due to the crystal temperature being somewhat lower than the measured value. These X-ray intensity data were collected before we adopted the practice of measuring the changes in crystal lattice parameters over a range of temperature so as to match the temperatures of the X-ray and neutron data collection (McMullan, Epstein, Ruble & Craven, 1979). However, this may not be a satisfactory explanation. Systematic differences in U_{ij} values have been found in other related structure determinations although the temperatures were believed to be matched within 5 K (Craven & McMullan, 1979; Craven & Benci, 1981). In these structures, as in barbital II, there are probably systematic errors in the intensity measurements due to the neglect of thermal diffuse scattering or to non-uniform intensity in the monochromated X-ray beam. The presence of systematic errors in U_{ij} values has a severe effect on the calculated charge density within about 0·3 Å of each atom center (Stewart, 1968), but this is attenuated in the valence-shell region.

For the X-ray refinements in the case of barbital II, the effect of the third-order temperature factor on a calculated structure factor with $\sin\theta/\lambda \sim 1{\cdot}0\ \text{Å}^{-1}$ is typically an order of magnitude less than that of the usual anisotropic temperature factor. The effect of systematic errors in c_{jkl} values should be correspondingly reduced. This is a further incentive for the determination of accurate c_{jkl} values from neutron diffraction data for reflections with large $\sin\theta/\lambda$.

Discussion

(*a*) *The distribution of net atomic charges*

The net valence charges (p_v) obtained for the pseudoatoms in barbital II (Table 3*b*)* are consistent with conventional notions regarding electronegativities. Thus, each O atom has an excess charge of 0·21 (3) e acquired from the carbonyl C atoms and the H-bonded H atom. However, it must be recognized that the magnitudes of such charge shifts are model-dependent, particularly with respect to the nature of the assumed charge-density radial functions. Presently, these are of the Slater-type. Also, the p_v parameters are strongly correlated with the corresponding radial parameters α. The correlation factors range from 0·58 to 0·81 except for the larger value (0·90) obtained for the N atom.

* A computer program limitation prevented the refinement of c_{jkl} parameters together with the charge-density parameters.

† Lists of observed and calculated X-ray structure factors, and un-normalized electron population parameters referred to crystal axes have been deposited with the British Library Lending Division as Supplementary Publication No. SUP 36724 (43 pp.). Copies may be obtained through The Executive Secretary, International Union of Crystallography, 5 Abbey Square, Chester CH1 2HU, England.

* The discussion refers to the second value given in Table 3(*a*) and (*b*) for each charge-density parameter. These values, which were obtained from the refinement including third-order temperature factors, were also used in obtaining Figs. 4, 5 and 6.

Most pseudoatoms in barbital II have a net charge which is significantly non-zero. In this respect, they differ from the charges observed in the related molecule of parabanic acid. The difference is attributed to the slightly larger values obtained for the radial parameters in barbital II, corresponding to a slight contraction of the pseudoatom charge distributions. In parabanic acid, the values for α were 3·25 (2), 3·89 (2), 4·40 (1) and 2·14 (6) bohr^{-1}, for C, N, O and H atoms respectively (Craven & McMullan, 1979). In barbital II, except for the N atom, the values (Table 3*a*) agree more closely with the standard values (3·44, 3·90, 4·50 and 2·48 bohr^{-1}) proposed by Hehre, Stewart & Pople (1969) on the basis of molecular-orbital calculations for selected small molecules. Ruble, Wang & Craven (1979) used these standard α values in deriving pseudoatom charges for barbital in four different crystal complexes with other molecules. Their refinements involved the *L*-shell projection method (Stewart, 1970) using only limited Cu $K\alpha$ X-ray diffraction data. The average p_v values for the four barbital molecules in these crystal complexes are in good agreement with those presently obtained (Table 3*b*), except for the N atoms, which had the average value p_v = 5·39 (4) as compared with 5·00 (4) e in barbital II. The difference may come from the strong correlation (0·91) already noted between α_N and p_v for N(3) in barbital II, and the rather large value $\alpha_N = 4{\cdot}05$ bohr^{-1}.

Comparisons of atomic charges are most meaningful when they involve pseudoatoms of the same element, having the same radial charge-density functions with the same α values. Thus in barbital II, there is no significant difference in the charges of the O atoms O(2) and O(4), although O(4) is H-bonded, while O(2) is not. It is of interest that the sequence of bonded atoms C(4)–C(5)–C(7)–C(8) shows an alternation in valence charges: 3·88 (3), 3·96 (3), 3·76 (4) and 3·87 (5) e. Although the alternation is only marginally significant in terms of the e.s.d.'s, a similar alternation can be seen in corresponding values (3·61, 4·08, 4·03, 4·08 e) given by Voet (1972) who carried out molecular-orbital calculations for barbital using the CNDO/2 approximation. Such a charge pattern may be an inductive effect due to the carbonyl O atom bonded to C(4). This would be consistent with the conclusions of Pople & Beveridge (1970) who noted the alternating charge patterns obtained from their CNDO/2 calculations for small hydrocarbons with O substituents.

The p_v values for the H atoms in barbital II show that there is a significant electronic charge depletion at the H-bonded atom H(3) compared with the H atoms of the methylene or methyl groups. Thus, for H(3), the charge is 0·88 (2) e, whereas for the H atoms in the C–H groups, the charge ranges from 1·04 (3) to 1·12 (3) e with an average value 1·09 e. Similar depletions are observed in the charge at H-bonded H atoms in 9-methyladenine (Craven & Benci, 1981) and in imidazole (Epstein, Ruble & Craven, 1982). These results are consistent with the simple electrostatic theory for the H bond, which requires the H atom to be relatively electropositive (Coulson & Danielsson, 1955).

(*b*) *The* H *pseudoatoms*

In barbital II, there is a distinctive aspherical distribution of charge density about each kind of pseudoatom, that is, about H, C(trigonal), C(tetrahedral), N and O atoms. For the H atoms, the deformation charge density is dominated by the dipole terms (Tables 3, 4). These deformations result in building up the charge density in the N–H or C–H bond region and in deshielding that side of the proton which is exposed to the molecular environment. This is consistent with the well known effect that in conventional X-ray refinements where H-atom positions are determined using spherical atomic scattering factors,

Table 4. *Atomic dipole moments*

These local dipole moments are derived from the dipole deformations of electronic charge density at each pseudoatom (Stewart, 1972). The explicit expression for the component of the atomic dipole moment along the x axis is $\mu_x = -5ed_x/(12\alpha)$ a.u. for non-H atoms or $\mu_x = -ed_x/(3\alpha)$ a.u. for H atoms with similar expressions for μ_y and μ_z. Here, e is the electron charge, α is the appropriate radial parameter from Table 3, and d_x, d_y, d_z are the dipole population parameters from Table 3 after transformation to local atomic axes.

For all atoms the local z axis is the normal to the ring plane on the side of the ethyl group which was chosen for the asymmetric unit (Table 3). For atoms C(2), O(2), C(5), C(7) and C(8), the x axis is parallel to the bond vector C(2)→O(2). For atoms N(3), H(3), C(4), O(4), the x axis is parallel to the appropriate extra-annular bond vector, N(3)→H(3) or C(4)→O(4). For the remaining H atoms, the x axis is along the appropriate C→H bond vector. The y axis at each atom is chosen to complete a right-handed Cartesian system.

μ values are in debye $\times 10^2$ (1 debye $\equiv 3{\cdot}336 \times 10^{-30}$ C m).

	$\lvert\mu\rvert$	μ_x	μ_y	μ_z	Angle $\mu \wedge x$
C(2)	44 (5)	−44 (5)	0	0	0°
O(2)	28 (3)	−28 (3)	0	0	0
N(3)	9 (5)	5 (3)	7 (3)	3 (3)	123
H(3)	113 (13)	112 (9)	10 (7)	0 (7)	175
C(4)	13 (6)	−4 (3)	−3 (3)	−12 (4)	71
O(4)	17 (4)	−11 (2)	−8 (2)	10 (2)	50
C(5)	10 (4)	10 (4)	0	0	180
C(7)	17 (8)	−15 (5)	6 (5)	−3 (5)	25
H(71)	142 (16)	142 (11)	−5 (7)	1 (8)	178
H(72)	106 (15)	106 (10)	2 (7)	−3 (8)	178
C(8)	40 (12)	−38 (7)	11 (7)	−6 (7)	18
H(81)	59 (22)	40 (13)	44 (12)	−1 (13)	132
H(82)	89 (22)	88 (12)	10 (11)	−5 (11)	173
H(83)	133 (20)	127 (13)	−18 (11)	−33 (11)	163

there is an apparent shortening of N–H and C–H bond lengths (Stewart, Davidson & Simpson, 1965). Compared with neutron values, these bonds seem to be shorter by about 0·1 Å (Hamilton & LaPlaca, 1968). However, when the proton positional and thermal parameters are fixed from neutron data, the X-ray data can then be used to obtain and compare the local dipole moments, as well as the net charges at different H atoms (Stewart, 1972).

The atomic dipole moments (Table 4) are significant for all H atoms, and are directed within 5° of the C–H or N–H bonds. Possible exceptions are for the H atoms of the terminal methyl group. However, the charge distribution for these atoms is less accurate because the protons have considerable r.m.s. thermal-vibrational amplitudes (~0·4 Å; MFC). Atomic dipole moments for H atoms in barbital C–H groups have values similar to those in cytosine monohydrate (Weber & Craven, 1982), 9-methyladenine (Craven & Benci, 1981) and imidazole (Epstein, Ruble & Craven, 1982). In these crystal structures, there are eight H atoms which are bonded to tetrahedral C atoms. They have a weighted mean value and e.s.d. of $\mu = 1{\cdot}07\ (27)$ debye. The distribution of atomic dipole moments for the seven H atoms bonded to trigonal C atoms is not significantly different, with $\mu = 0{\cdot}94\ (23)$ debye. For all 15 H atoms, $\mu = 1{\cdot}02\ (27)$ debye.

For the H atoms in N–H groups, the local electronic dipole in combination with the net electronic charge depletion should favor a stronger H-bonding interaction by allowing closer intermolecular approach to the deshielded proton. At present, barbital II and parabanic acid are the only structures with N–H···O=C interactions for which data are available. For these H bonds, the H···O distances are similar in barbital II (1·83 Å) and in parabanic acid (1·89, 1·82 Å) and so are the corresponding values μ = 1·13 (13), 1·33 (29), 1·32 (29) debye, respectively.

(c) *Pseudoatoms of the ring*

For the trigonally bonded ring atoms N(3), C(2) and C(4), the important charge-density deformation terms are the octapoles o_1 and o_2 and the quadrupole terms q_1 and q_5 (Table 3*b*). These terms all have angular functions with symmetry about axes normal to the ring plane and passing through the atom center. The axial symmetry is threefold for the octapoles o_1 and o_2, twofold for the quadrupole q_1 and cylindrical for q_5. The terms o_1, o_2 and q_1 are the major contributors to the excess of charge density which occurs in the σ region of the ring bonds (Figs. 4 and 5). The positive value of q_5 for atom N(3) gives an excess of electron charge near N(3) in the π-bonding regions above and below the ring plane and a deficiency of charge in the σ-bonding region close to the ring plane. For the C atoms, the opposite sign for q_5 gives the reverse effect.

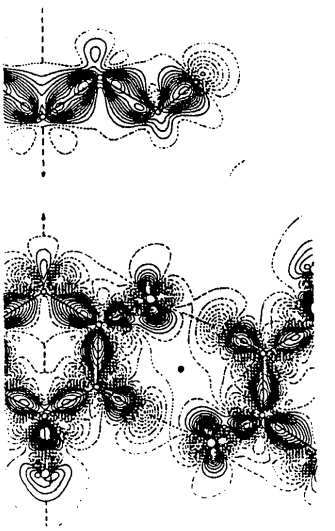

Fig. 4. Map of deformations in the valence charge density resulting from the final refinement which included third-order temperature factors. The density is shown below in the section parallel to (10$\bar{1}$) through the H-bonding region and above in the section through the plane of the ethyl-group C atoms, which is almost perpendicular to the plane of the ring system. Contours and e.s.d.'s are as in Fig. 3.

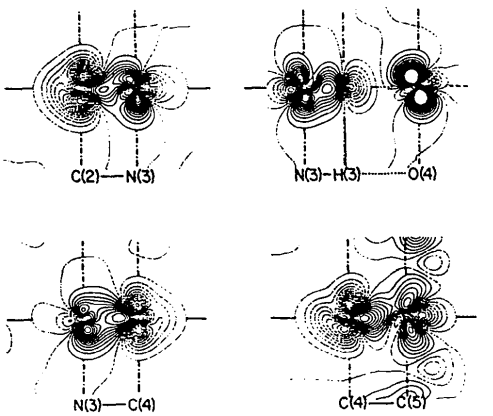

Fig. 5. Sections showing the deformation density in the ring bonds and the H bond. In each case, the normal to the plane of the ring is directed vertically in the page. Sections are through the centers of bonded pairs of atoms, or N(3) and O(4) in the case of the H bond.

In the C–N bonds, the combination of these deformations may be considered as a polarization of charge toward the C atom in the σ region and towards the N atom in the π region (Fig. 5). Similar features were observed for the C–N bonds in parabanic acid (Craven & McMullan, 1979). The deformation density at the tetrahedral ring atom C(5) is similar to that at N(3) except for the large value for the term o_5, which displaces charge density into the C(5)–C(7) bond.

(*d*) *The oxygen pseudoatoms*

The deformation density around the carbonyl O atoms consists of twin lobes of excess electronic charge density which are directed approximately at right angles to the C—O bond, and a region deficient in charge density which is along the C—O bond (Figs. 4, 6). In barbital II, the lobes of excess density at both O atoms occur above and below the plane of the ring so that they are almost opposite the corresponding lobes of charge deficiency at the carbonyl C atoms (Fig. 6). Thus, the C—O bonds are polarized like the C—N bonds, but more strongly, with electronic charge displaced towards the C atoms in the σ region and towards the O atoms in the π region.

A remarkable feature at different amide O atoms is the variability observed in the orientation of the twin lobes with respect to rotation about an axis close to the C—O bond. In the crystal structures of diformohydrazide (Tanaka, 1978; Hope & Ottersen, 1979; Eisenstein, 1979) and for two of the three carbonyl groups in parabanic acid (Craven & McMullan, 1979) the O lobes are close to the plane of the amide group. This is the orientation predicted for an isolated formamide molecule (Stevens, Rys & Coppens, 1978) from *ab initio* molecular-orbital calculations with an extended basis set. These lobes were characterized as lone-pair electron density for the O atom in the sp^2 hybridization state. However, in other amide groups, the O lobes are twisted out of the amide plane. The effect was first observed for acetamide in the crystal complex with allenedicarboxylic acid (Berkovitch-Yellin, Leiserowitz & Nader, 1977) and has since been noted in the crystal structures of formamide (Stevens, Rys & Coppens, 1978), and parabanic acid (Craven & McMullan, 1979) and is presently observed at both O atoms in barbital II (Fig. 6). In this orientation, the lobes are more readily characterized as π-bonding features.

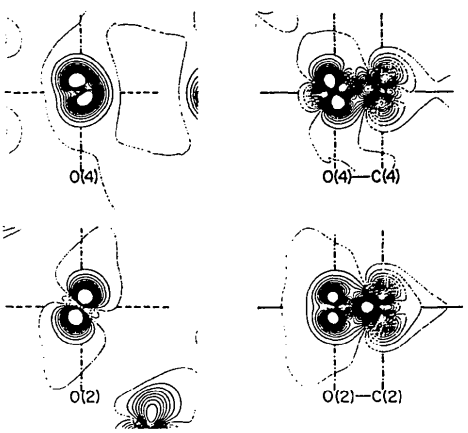

Fig. 6. Sections showing the carbonyl-group deformation density as obtained from the final refinement. In each case, the normal to the plane of the ring is directed vertically in the page. On the left are sections through the O-atom centers and normal to the C—O bond. On the right are sections through the C- and O-atom centers. Contours are at intervals of 0·05 e Å^{-3}. Maximum values of electronic charge density are 1·21 (8) and 1·14 (8) e Å^{-3} near atoms O(2) and O(4) respectively. The map is of static charge density from which has been subtracted a promolecule consisting of an assembly of neutral spherical pseudoatoms. Thus the density consists of all the deformation terms together with spherical terms having populations ($p_v - Z_v$) where Z_v is the number of valence electrons in the neutral pseudoatom, *i.e.* $Z_v = 4$ for C atoms, *etc.*

The orientation of the lobes with respect to the amide plane does not appear to be related to the C—O bond length. Thus in formamide and diformohydrazide, the bond lengths are the same (1·239 Å) within the error estimates (0·004 Å), although the lobe orientations are in-plane for one and out-of-plane for the other (formamide). Also, the orientation does not appear to be related to the H-bonding arrangement, since barbital has the O(4) atom H-bonded, while O(2) is not, yet both O atoms have lobes twisted out of the amide plane. Furthermore, atom O(2) in parabanic acid is not H-bonded, yet the lobes are in the amide plane. The C—O bond lengths in barbital and parabanic acid are all relatively short, ranging from 1·203 to 1·226 Å (σ = 0·002 Å).

It might be considered that these various orientations of the O-atom deformation density are due to a defective deconvolution of the static charge density from the atomic thermal motion in the crystal structure. However, this is not supported by recent results of Swaminathan & Craven (1982) who have carried out separate multipole refinements using X-ray data collected for oxamide at 298, 203 and 123 K. The magnitude of the O-atom deformation features increases significantly as the temperature decreases. However, there is little change in the orientation of the lobes, which are found to be twisted out of the amide plane.

At present, there is no satisfactory explanation for this effect. The variability of the deformation density at amide O atoms appears to represent a significant discrepancy between the theoretical and experimental determination of charge density for these compounds.

(*e*) *The molecular dipole moment*

The molecular dipole moment has been calculated following Stewart (1972). It was found that the contribution +4·3 (1·1) debye coming from the distribution of net charges at the atomic centers, is almost cancelled by the contribution from the sum of local atomic dipoles, −3·6 (4) debye. The resultant molecular dipole moment, which is directed along the molecular and crystallographic twofold axis, is 0·7 (1·2) debye. The negative charge displacement is towards atom C(5) and the positive is towards O(2). The result is consistent with the more accurate value

1·13 (1) debye reported by Soundararajan (1958) for barbital in dioxane solution (0·01 mol fraction).

This work was supported by grant GM-22548 from the National Institutes of Health. Technical assistance was provided by Dr John R. Ruble, Ms Irene Marinakos and Mr Paul Kruth.

References

BENTLEY, J. & STEWART, R. F. (1974). *Acta Cryst.* A**30**, 60–67.

BERKOVITCH-YELLIN, Z., LEISEROWITZ, L. & NADER, F. (1977). *Acta Cryst.* B**33**, 3670–3677.

BIDEAU, J. P., LEROY, F. & HOUSTY, J. (1969). *C. R. Acad. Sci. Sér. C*, **268**, 1590–1592.

BUSING, W. R. & LEVY, H. A. (1957). *Acta Cryst.* **10**, 180–182.

CLEMENTI, E. (1965). *IBM J. Res. Dev. Suppl.* **9**, 2.

COULSON, C. A. & DANIELSSON, U. (1955). *Ark. Fys.* **8**, 239–255.

CRAVEN, B. M. & BENCI, P. (1981). *Acta Cryst.* B**37**, 1584–1591.

CRAVEN, B. M., CUSATIS, C., GARTLAND, G. L. & VIZZINI, E. A. (1973). *J. Mol. Struct.* **16**, 331–342.

CRAVEN, B. M. & MCMULLAN, R. K. (1979). *Acta Cryst.* B**35**, 934–945.

CRAVEN, B. M. & VIZZINI, E. A. (1971). *Acta Cryst.* B**27**, 1917–1924.

CRAVEN, B. M., VIZZINI, E. A. & RODRIGUES, M. M. (1969). *Acta Cryst.* B**25**, 1978–1993.

CRAVEN, B. M. & WEBER, H.-P. (1977). *The 'POP' Least-Squares Refinement Procedure.* Tech. Rep., Department of Crystallography, Univ. of Pittsburgh.

EISENSTEIN, M. (1979). *Acta Cryst.* B**35**, 2614–2625.

EPSTEIN, J., RUBLE, J. R. & CRAVEN, B. M. (1982). *Acta Cryst.* B**38**, 140–149.

FREUDENTHAL, R. I. & MARTIN, J. (1975). *J. Pharmacol. Exp. Ther.* **193**, 664–668.

GARTLAND, G. L. & CRAVEN, B. M. (1974). *Acta Cryst.* B**30**, 980–987.

HAMILTON, W. C. (1974). *International Tables for X-ray Crystallography*, Vol IV, pp. 285–310. Birmingham: Kynoch Press.

HAMILTON, W. C. & LAPLACA, S. J. (1968). *Acta Cryst.* B**24**, 1147–1156.

HAMILTON, W. C., ROLLETT, J. S. & SPARKS, R. A. (1965). *Acta Cryst.* **18**, 129–130.

HANSEN, N. K. & COPPENS, P. (1978). *Acta Cryst.* A**34**, 909–921.

HEHRE, W. J., STEWART, R. F. & POPLE, J. A. (1969). *J. Chem. Phys.* **51**, 2657–2664.

HOPE, H. & OTTERSEN, T. (1979). *Acta Cryst.* B**35**, 370–372.

HSU, I. N. & CRAVEN, B. M. (1974*a*). *Acta Cryst.* B**30**, 988–993.

HSU, I. N. & CRAVEN, B. M. (1974*b*). *Acta Cryst.* B**30**, 1299–1304.

JOHNSON, C. K. & LEVY, H. A. (1974). *International Tables for X-ray Crystallography*, Vol. IV, pp. 311–336. Birmingham: Kynoch Press.

KIM, S. H. & RICH, A. (1968). *Proc. Natl Acad. Sci. USA*, **60**, 402–408.

MCMULLAN, R. K., EPSTEIN, J., RUBLE, J. R. & CRAVEN, B. M. (1979). *Acta Cryst.* B**35**, 688–691.

MCMULLAN, R. K., FOX, R. O. & CRAVEN, B. M. (1978). *Acta Cryst.* B**34**, 3719–3722.

NICOLL, R. (1978). *Psychopharmacology: A Generation of Progress*, edited by M. A. LIPTON, A. DIMASCIO & K. F. KILLAM, pp. 1337–1348. New York: Raven Press.

POPLE, J. A. & BEVERIDGE, D. L. (1970). *Approximate Molecular Orbital Theory*, p. 125. New York: McGraw-Hill.

RUBLE, J. R., WANG, A. C. & CRAVEN, B. M. (1979). *J. Mol. Struct.* **51**, 229–237.

SOUNDARARAJAN, S. (1958). *Trans. Faraday Soc.* **54**, 1147–1150.

STEVENS, E. D., RYS, J. & COPPENS, P. (1978). *J. Am. Chem. Soc.* **100**, 2324–2328.

STEWART, R. F. (1968). *Acta Cryst.* A**24**, 497–505.

STEWART, R. F. (1970). *J. Chem. Phys.* **53**, 205–213.

STEWART, R. F. (1972). *J. Chem. Phys.* **57**, 1664–1668.

STEWART, R. F. (1976). *Acta Cryst.* A**32**, 565–574.

STEWART, R. F., DAVIDSON, E. R. & SIMPSON, W. T. (1965). *J. Chem. Phys.* **42**, 3175–3187.

SWAMINATHAN, S. & CRAVEN, B. M. (1982). *Acta Cryst.* To be submitted.

TANAKA, K. (1978). *Acta Cryst.* B**34**, 2487–2494.

VOET, D. (1972). *J. Am. Chem. Soc.* **94**, 8213–8222.

WANG, B. C. & CRAVEN, B. M. (1971). *J. Chem. Soc. Chem. Commun.* pp. 290–291.

WEBER, H.-P. & CRAVEN, B. M. (1982). *Acta Cryst.* To be submitted.

WILLIAMS, P. P. (1974). *Acta Cryst.* B**30**, 12–17.

WILLIS, B. T. M. & PRYOR, A. W. (1975). *Thermal Vibrations in Crystallography*, pp. 198–203. Cambridge Univ. Press.